

# Supporting Information

## Application of Transient IR Spectroscopy to Investigate the Role of Gold in Ethanol Gas Sensing over Au/SnO<sub>2</sub>

Maximilian Pfeiffer, Christian Hess\*

TU Darmstadt, Eduard Zintl Institute of Inorganic and Physical Chemistry, Alarich-Weiss-Str. 8, 64287 Darmstadt, Germany

\*e-mail: christian.hess@tu-darmstadt.de

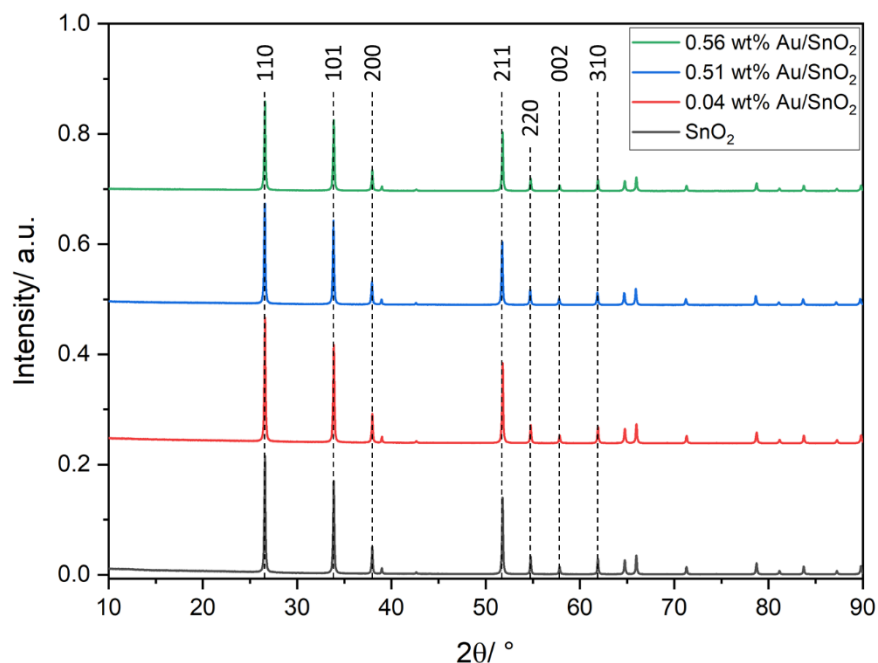


Figure S1. X-ray powder diffractograms of the samples using Cu K $\alpha$ -radiation (1.5406 Å, 40 kV, 40 mA).

**Table S1.** Composition of bare and gold-loaded tin oxide materials used in this work.

Sample name	XPS						ICP-OES
	x(C)/ at%	x(O)/ at%	x(Sn)/ at%	x(Au)/ at%	w(Au)/ wt%	O/Sn	w(Au)/ wt%
SnO <sub>2</sub>	5.2	59.7	35.1	0.0	0.00	1.70	0.00
0.04 wt% Au/SnO <sub>2</sub>	13.0	56.3	30.7	0.0	0.00	1.83	0.04
0.51 wt% Au/SnO <sub>2</sub>	7.2	58.6	33.7	0.5	1.92	1.74	0.51
0.56 wt% Au/SnO <sub>2</sub>	9.1	57.2	33.2	0.6	2.17	1.72	0.56

**Table S2.** Mean crystallite sizes and specific surface areas of bare and gold-loaded tin oxide samples, as determined from X-ray diffraction and N<sub>2</sub> physisorption measurements.

Probe	Mean crystallite size <i>d</i> / nm	Specific surface area/ m <sup>2</sup> ·g <sup>-1</sup>
SnO <sub>2</sub>	59.0	25.0
0.04 wt% Au/SnO <sub>2</sub>	57.0	17.3
0.51 wt% Au/SnO <sub>2</sub>	59.1	19.8
0.56 wt% Au/SnO <sub>2</sub>	57.0	25.5

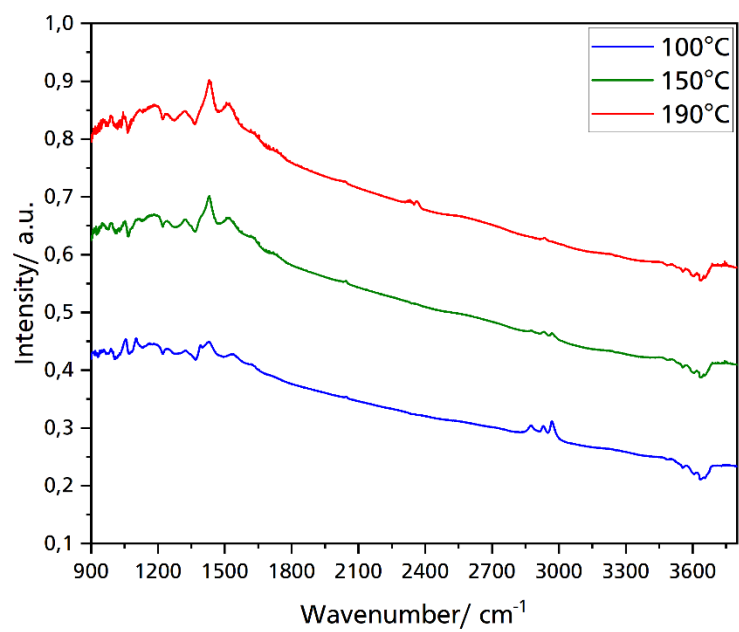


**Figure S2.** Exemplary DRIFT spectrum of 0.56 wt% Au/SnO<sub>2</sub> during exposure to 500 ppm ethanol at operating temperatures of 100°C, 150°C, and 190°C.

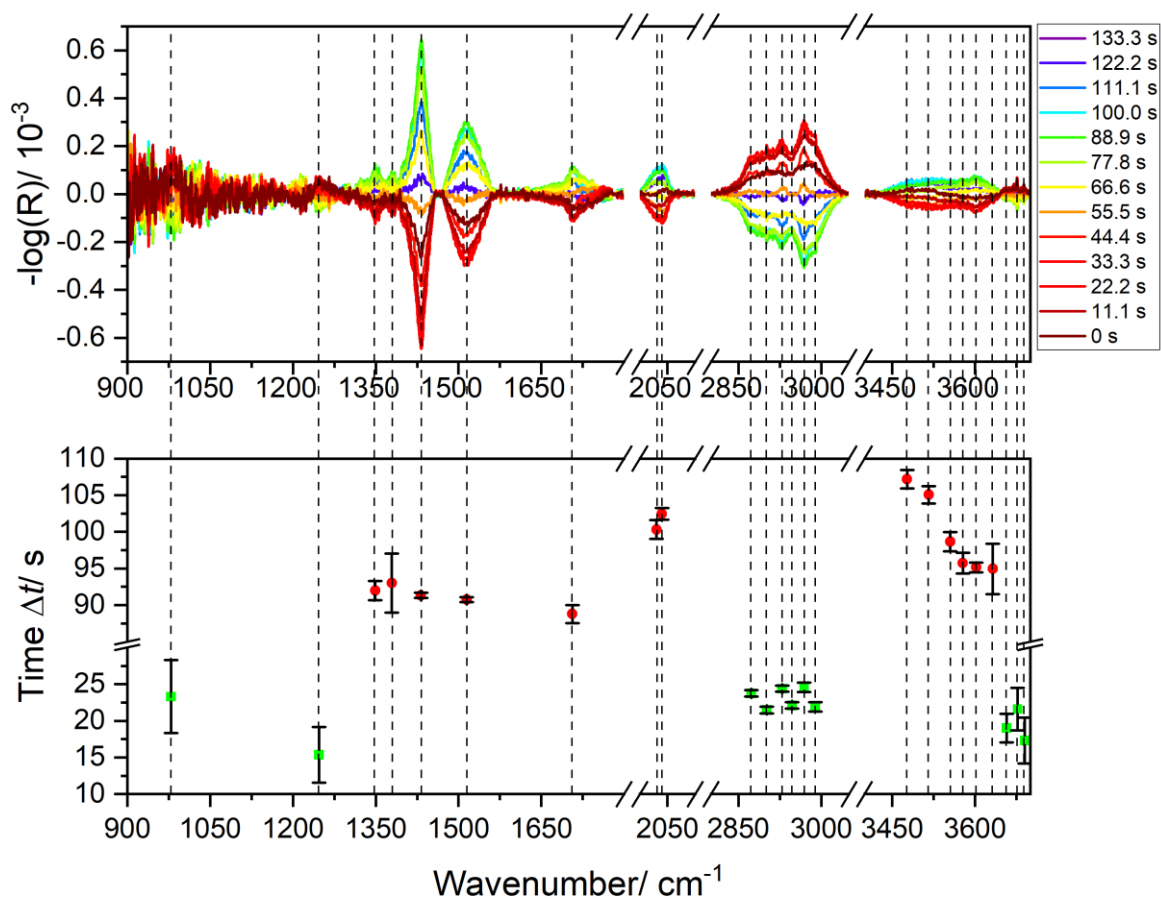


**Figure S3.** Temporal analysis of PSD spectra for 0.56 wt% Au/SnO<sub>2</sub> during pulsing of 500 ppm ethanol in synthetic air at 150°C. Time values  $\Delta t$  (bottom panel) were calculated from the phase angles at maximum band intensity. Dashed lines indicate the maxima of observed features and their corresponding time values. Time values in the first half-period are colored green, those in the second half-period are colored red. The error bars show the standard deviation of the time values  $\Delta t$  within the range of  $\pm 5 \text{ cm}^{-1}$  with respect to the position of the maximum.

**Table S3.** Band assignment based on results of time-resolved DRIFTS measurements and observations in the literature;  
T: terminal; B: bridged.

Band position/ cm <sup>-1</sup>	Band assignment	Literature
934	$\delta(\text{Sn-OH})(\text{T})$	1-3
979	$\delta(\text{Sn-OH})(\text{T})$	1,4,5
1100	$\nu(\text{C-O})$ ethoxy	6,7
1247	$\delta(\text{Sn-OH})(\text{T})$	2,4,5
1349	$\nu_s(\text{COO})$ carboxylate	4,8,9
1379	$\nu_s(\text{COO})$ carbonate	3,4,8,9
1432	$\nu_{as}(\text{COO})$ carbonate	3,4,8,9
1515	$\nu_{as}(\text{COO})$ carboxylate	4,8,9
1626	$\delta(\text{HOH}) \text{H}_2\text{O}_{\text{ads}}$	1,8,10,11
1706	$\nu(\text{C=O})$ acetaldehyde)	12,13
2040	$\text{CO-Au}^{\delta-}$	14-16
2349	$\nu_{as}(\text{OCO}) \text{CO}_{2,\text{gas}}$	3,17-19
2873	$\nu_s(\text{CH}_3)$ acetate, ethoxy $\nu(\text{C-H})$ formate	12,14,20-22
2901	$\nu_{as}(\text{CH}_2)$ adsorbed ethanol	12,14,20-22
2929	$\nu_{as}(\text{CH}_2)$ ethoxy	12,14,20-22
2947	$\nu_{as}(\text{CH}_2)$ ethanol	12,14,20-22
2969	$\nu_{as}(\text{CH}_3)$ acetate, ethoxy $\nu(\text{C-H})$ formate	12,14,20-22
2989	$\nu_{as}(\text{CH}_3)$ ethanol	12,14,20-22
3460	$\nu(\text{OH})(\text{B})$	1,10,23-25
3555	$\nu(\text{OH})(\text{B})$	1,10,23-25
3604	$\nu(\text{OH})(\text{T})$	1,10,23-25
3631	$\nu(\text{OH})(\text{T})$	1,10,23-25
3636	$\nu(\text{OH})(\text{T})$	1,10,23-25
3652	$\nu(\text{OH})(\text{T})$	1,10,23-25
3673	$\nu(\text{OH})(\text{T})$	1,10,23-25

## References

- (1) Degler, D.; Junker, B.; Allmendinger, F.; Weimar, U.; Barsan, N. Investigations on the Temperature-Dependent Interaction of Water Vapor with Tin Dioxide and Its Implications on Gas Sensing. *ACS Sens.* **2020**, *5*, 3207–3216.
- (2) Orel, B.; Lavrenčič-Štankgar, U.; Crnjak-Orel, Z.; Bukovec, P.; Kosec, M. Structural and FTIR spectroscopic studies of gel-xerogel-oxide transitions of SnO<sub>2</sub> and SnO<sub>2</sub>:Sb powders and dip-coated films prepared via inorganic sol-gel route. *J. Non-Cryst. Solids* **1994**, *167*, 272–288.
- (3) Harbeck, S.; Szatvanyi, A.; Barsan, N.; Weimar, U.; Hoffmann, V. DRIFT studies of thick film un-doped and Pd-doped SnO<sub>2</sub> sensors: temperature changes effect and CO detection mechanism in the presence of water vapour. *Thin Solid Films* **2003**, *436*, 76–83.
- (4) Koziej, D.; Thomas, K.; Barsan, N.; Thibault-Starzyk, F.; Weimar, U. Influence of annealing temperature on the CO sensing mechanism for tin dioxide based sensors—Operando studies. *Catal. Today* **2007**, *126*, 211–218.
- (5) Thornton, E. W.; Harrison, P. G. Tin oxide surfaces. Part 1.—Surface hydroxyl groups and the chemisorption of carbon dioxide and carbon monoxide on tin(IV) oxide. *J. Chem. Soc., Faraday Trans. 1* **1975**, *71*, 461.
- (6) Song, H.; Bao, X.; Hadad, C. M.; Ozkan, U. S. Adsorption/Desorption Behavior of Ethanol Steam Reforming Reactants and Intermediates over Supported Cobalt Catalysts. *Catal. Lett.* **2011**, *141*, 43–54.
- (7) Chiericato, A.; Velasquez Ochoa, J.; Bandinelli, C.; Fornasari, G.; Cavani, F.; Mella, M. On the chemistry of ethanol on basic oxides: revising mechanisms and intermediates in the Lebedev and Guerbet reactions. *ChemSusChem* **2015**, *8*, 377–388.
- (8) Harrison, P. G.; Guest, A. Tin oxide surfaces. Part 18.—Infrared study of the adsorption of very low levels (20–50 ppm) of carbon monoxide in air on to tin (IV) oxide gel. *J. Chem. Soc., Faraday Trans. 1* **1989**, *85*, 1897.
- (9) Wicker, S.; Guiltat, M.; Weimar, U.; Hémerlyck, A.; Barsan, N. Ambient Humidity Influence on CO Detection with SnO<sub>2</sub> Gas Sensing Materials. A Combined DRIFTS/DFT Investigation. *J. Phys. Chem. C* **2017**, *121*, 25064–25073.
- (10) Amalric-Popescu, D.; Bozon-Verduraz, F. Infrared studies on SnO<sub>2</sub> and Pd/SnO<sub>2</sub>. *Catal. Today* **2001**, *70*, 139–154.
- (11) Christensen, P. A.; Attidekou, P. S.; Egdell, R. G.; Maneelok, S.; Manning, D. A. C. An in situ FTIR spectroscopic and thermogravimetric analysis study of the dehydration and dihydroxylation of SnO<sub>2</sub>: the contribution of the (100), (110) and (111) facets. *Phys. Chem. Chem. Phys.* **2016**, *18*, 22990–22998.
- (12) Raskó, J.; Hancz, A.; Erdőhelyi, A. Surface species and gas phase products in steam reforming of ethanol on TiO<sub>2</sub> and Rh/TiO<sub>2</sub>. *Appl. Catal. A-Gen* **2004**, *269*, 13–25.

- (13) Christensen, P. A.; Mashhadani, Z. T. A. W.; Md Ali, A. H. B. In situ FTIR studies on the oxidation of isopropyl alcohol over SnO<sub>2</sub> as a function of temperature up to 600°C and a comparison to the analogous plasma-driven process. *Phys. Chem. Chem. Phys.* **2018**, *20*, 9053–9062.
- (14) Tan, T. H.; Scott, J.; Ng, Y. H.; Taylor, R. A.; Aguey-Zinsou, K.-F.; Amal, R. C–C Cleavage by Au/TiO<sub>2</sub> during Ethanol Oxidation: Understanding Bandgap Photoexcitation and Plasmonically Mediated Charge Transfer via Quantitative in Situ DRIFTS. *ACS Catal.* **2016**, *6*, 8021–8029.
- (15) Wang, J.; Kispersky, V. F.; Nicholas Delgass, W.; Ribeiro, F. H. Determination of the Au active site and surface active species via operando transmission FTIR and isotopic transient experiments on 2.3wt.% Au/TiO<sub>2</sub> for the WGS reaction. *J. Catal.* **2012**, *289*, 171–178.
- (16) Boccuzzi, F.; Chiorino, A.; Manzoli, M.; Andreeva, D.; Tabakova, T. FTIR Study of the Low-Temperature Water–Gas Shift Reaction on Au/Fe<sub>2</sub>O<sub>3</sub> and Au/TiO<sub>2</sub> Catalysts. *J. Catal.* **1999**, *188*, 176–185.
- (17) Atkins, P. W.; Paula, J. de; Bär, M. *Physikalische Chemie*, 5. Aufl.; Wiley-VCH, Weinheim, 2013.
- (18) Degler, D.; Rank, S.; Müller, S.; Pereira de Carvalho, H. W.; Grunwaldt, J.-D.; Weimar, U.; Barsan, N. Gold-Loaded Tin Dioxide Gas Sensing Materials: Mechanistic Insights and the Role of Gold Dispersion. *ACS Sens.* **2016**, *1*, 1322–1329.
- (19) Gonugunta, P.; Dugulan, A. I.; Bezemer, G. L.; Brück, E. Role of surface carboxylate deposition on the deactivation of cobalt on titania Fischer-Tropsch catalysts. *Catal. Today* **2021**, *369*, 144–149.
- (20) Zhang, S.; Song, P.; Yan, H.; Wang, Q. Self-assembled hierarchical Au-loaded In<sub>2</sub>O<sub>3</sub> hollow microspheres with superior ethanol sensing properties. *Sens. Actuators B* **2016**, *231*, 245–255.
- (21) Sänze, S.; Gurlo, A.; Hess, C. Monitoring Gas Sensors at Work: Operando Raman-FTIR Study of Ethanol Detection by Indium Oxide. *Angew. Chem. Int. Ed.* **2013**, *52*, 3607–3610.
- (22) Elger, A.-K.; Hess, C. Elucidating the Mechanism of Working SnO<sub>2</sub> Gas Sensors Using Combined Operando UV/Vis, Raman, and IR Spectroscopy. *Angew. Chem. Int. Ed.* **2019**, *58*, 15057–15061.
- (23) Ivanovskaya, M.; Ovodok, E.; Gaevskaya, T.; Kotsikau, D.; Kormosh, V.; Bilanych, V.; Micusik, M. Effect of Au nanoparticles on the gas sensitivity of nanosized SnO<sub>2</sub>. *Mat. Chem. Phys.* **2021**, *258*, 123858.
- (24) Großmann, K.; Barsan, N.; Weimar, U. Operando DRIFT Measurements on a tin dioxide based gas sensor. *Procedia Eng.* **2010**, *5*, 119–122.
- (25) Hübner, M.; Koziej, D.; Bauer, M.; Barsan, N.; Kvashnina, K.; Rossell, M. D.; Weimar, U.; Grunwaldt, J.-D. The Structure and Behavior of Platinum in SnO<sub>2</sub> -Based Sensors under Working Conditions. *Angew. Chem. Int. Ed.* **2011**, *50*, 2841–2844.